KunturSat: Design and Development of a Picosatellite for the CanSat France 2024 Competition

Luis Fernando Aiquipa Moreno¹, Juan Miguel Villanueva Orellana¹, Marco Antonio Rodriguez Adriano¹, Felixjesus Ramirez Tarazona^{1,2}, Katherine Karla Roman Meza¹, Roxana Yesenia Pastrana Alta^{1,*}

- 1. Universidad Nacional de Ingeniería 🏟 Facultad de Ciencias Laboratorio de Química Bioinorgánica en Medicina y Medio Ambiente Lima Peru.
- 2. Universidad Tecnológica del Perú 🐯 Facultad de Mecánica Ingeniería Mecánica Lima Peru.
- *Correspondence author: rpatranaa@uni.edu.pe

ABSTRACT

This paper presents the design, development, and validation of KunturSat, a picosatellite developed for the CanSat France 2024 competition. KunturSat integrates multiple technological innovations, including a flag deployment system, precise descent control via a 9-cell paraglider, and a biodegradable marking mechanism using purple corn extract (*Zea mays* var. *amilácea* (L.)). The structural design utilizes lightweight, high-strength materials, such as Ripstop nylon, and employs advanced 3D printing techniques, ensuring both durability and flight efficiency. A comprehensive series of tests was conducted to evaluate its performance, including vibration analysis, communication tests, support deployment trials, free-fall simulations, and drone-based launches. These assessments validated the mechanical, electronic, and telemetry subsystems under real-flight conditions. The results confirmed KunturSat's effectiveness in executing its primary mission of biodegradable surface marking, alongside its secondary missions of vertical stabilization and flag deployment. Identified improvements include reinforcement of structural components to enhance resilience in adverse conditions. KunturSat contributes to the aerospace sector as an innovative and sustainable platform, serving as a foundation for future picosatellites with autonomous descent control and advanced deployment mechanisms. Additionally, it underscores the importance of STEM education (science, technology, engineering, and mathematics) and accessible aerospace technologies in fostering engineering expertise.

Keywords: Small satellite technology; Deployment mechanism; Biomarkers; Descent trajectories.

INTRODUCTION

In recent decades, the launch of small satellites has increased significantly, where the term small satellite is somewhat arbitrarily defined as a spacecraft with an upper mass limit in the range of a few hundred kilograms, contributing to various scientific and engineering disciplines (Millan *et al.* 2019; Song *et al.* 2024). Their main advantage lies in their low cost, which enables scientific advancements in short periods, making them an attractive option for educational and research institutions (Kopacz *et al.* 2020). Although the complexity of small satellites may vary depending on their size and assigned mission, they are generally more economical than large satellites due to reduced transportation and launch costs, as well as lower safety requirements during liftoff (Nag *et al.* 2014; Sweeting 2018).

Received: Mar. 14, 2025 | Accepted: June 06, 2025 | Peer Review History: Single Blind Peer Review.

Section editor: Paulo Renato Silva (1)



One of the most interesting initiatives for training young people in the aerospace and space sector is the development of CanSattype picosatellites (Contente and Galvão 2022). The CanSat is an autonomous device that simulates a small satellite capable of carrying out scientific and research missions. It is based on the idea of designing, within a reduced volume equivalent to a soda can, a payload similar to that of a satellite. Originally 330 mL, this volume can be increased up to 1 L. CanSats are composed of various systems depending on the assigned mission and are used in institutions worldwide to motivate and provide a solid foundation for students interested in satellite development (Chun *et al.* 2023). Numerous CanSat projects have been developed to address different challenges and objectives, such as designing and developing a CanSat for atmospheric pollution monitoring (Swayampakula *et al.* 2024) and air quality assessment (Botero *et al.* 2023). Additionally, experimental CanSat platforms have been created for functional verification of mechanisms (Bhattarai *et al.* 2021), methods, and studies, as well as variations of Rover-Back prototypes (Aydemir *et al.* 2011), which allow for more applications and improvements through the use of wheels in kinematic models (Aly *et al.* 2013; Moreno *et al.* 2023).

CanSats are also powerful tools for driving innovation, enabling students and professionals to efficiently solve specific problems within short timeframes through international competitions. One of the most notable events is C'Space, an international CanSat competition organized by Planète Sciences and the Centre National d'Études Spatiales, aimed at promoting education and research. In this competition, CanSat picosatellites carry out their missions during descent and landing, using drones or mini-rockets as launch platforms.

This article presents the design and development of a CanSat-type picosatellite called KunturSat, where "kuntur" means "condor" in Quechua, and "sat" is derived from "satellite." The project includes four main mechanisms designed to meet the requirements of the CanSat France 2024 competition. This work presents a compact and low-cost educational satellite platform that integrates descent control, mechanical deployment, environmental monitoring systems, and release systems, offering a valuable foundation for student-led aerospace development initiatives. Based on the results obtained and the competition evaluation, this work contributes to:

- Design and prototyping of a CanSat with autonomous descent control for the fulfillment of specific missions.
- Data analysis after the picosatellite's flight as a test and experimental verification.
- A starting point for students and beginner enthusiasts in the design and construction of a CanSat mission requirements.

In this section, the main mission and the two secondary missions selected for the KunturSat project are described. The CanSat was launched from a drone provided by the competition at an altitude of 150 meters. The mission objectives were accomplished by three main systems: the mechanical system, the telemetry system, and the electrical and electronic system. Within the mechanical system, three key mechanisms were developed: the "liquid release mechanism," which used a screw conveyor and balloons filled with purple corn extract attached to the bottom of the CanSat to mark the ground surface, fulfilling the main mission of biodegradable marking; the "vertical descent mechanism," designed with four supports that ensured the stability of the CanSat upon landing, guaranteeing the success of the first secondary mission; and the "flag deployment mechanism," which used a servomotor to deploy a flag, ensuring that it remained elevated and did not touch the CanSat, fulfilling the second secondary mission. The telemetry system was responsible for transmitting real-time data during descent and after landing, allowing mission performance monitoring and recording information such as the Global Positioning System (GPS) position of the target, which was useful for fulfilling the main mission since the competition provided the exact location of the target to be marked. Meanwhile, the electrical and electronic system ensured the proper functioning of the mechanisms and sensors, supplying the necessary power for system deployment and data transmission to the ground station. Together, these systems worked in an integrated manner to ensure the success of the selected missions, which are detailed below.

MAIN MISSION: SURFACE MARKING WITH BIODEGRADABLE MATERIAL

The main mission was to cover the largest possible area on a surface during the landing of the CanSat using an ecofriendly material, such as biodegradable paint. Each marked area earned points, which were assigned according to the zones defined on an A0-sized target (Annex). The points corresponding to each zone were clearly indicated. To achieve this objective, one or multiple areas on the board were marked, each contributing to the total accumulated score, with a maximum of 50 points evaluated 5 minutes after landing. The highest concentration of marks was located at the center of the target point, while the size of the marks progressively decreased as they moved away from the center. The GPS position of the target point was 43°13'16.0"N, 0°03'09.0"W.



In this regard, the material used was purple corn extract ($\it Zea\ mays\ var.\ amilácea\ (L.)$), belonging to the Poaceae family (Urquizo and Sánchez 2019). This extract, obtained by boiling the kernels and cobs of Peruvian purple corn, is the main ingredient of *chicha morada*, a traditional national beverage of great cultural significance. Its selection was based on its coloring properties, derived from a natural pigment known as cyanidin-3- β -glucoside, which allowed the creation of visible marks (Zhou *et al.* 2024). The liquid was stored in balloons attached to the bottom of the structure, which were pierced by needles connected to a component activated by a screw conveyor, forming the so-called liquid release mechanism, which is described later when addressing the design of the system.

FIRST SECONDARY MISSION: MAINTENANCE OF VERTICAL POSITION

The first secondary mission aimed to keep the CanSat in a vertical position for at least 3 minutes after landing, considering the irregular nature of the terrain. This requirement emphasized the mechanical and structural stability of the CanSat design to withstand external disturbances and ensure its balance.

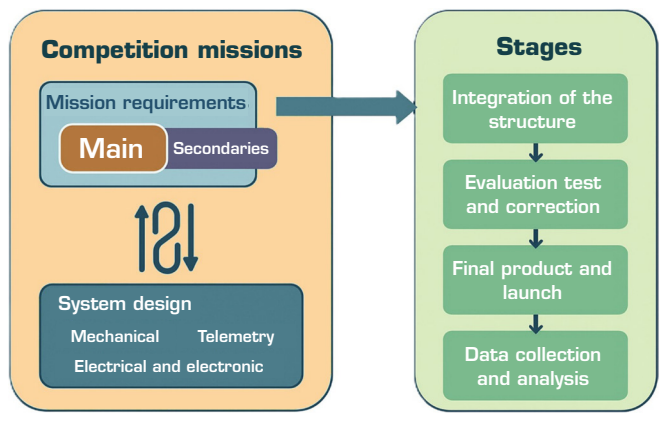
In this context, the prototyping of a mechanism was proposed, named the vertical descent mechanism, consisting of four supports. Its operation was governed by a device called a screw conveyor, which transmitted motion between perpendicular axes through a two-component system: the screw (with helical teeth) and a circular gear known as a worm wheel.

SECOND SECONDARY MISSION: FLAG DEPLOYMENT

The second secondary mission consisted of deploying a flag of at least $5 \text{ cm} \times 8 \text{ cm}$, ensuring that it remained elevated without touching the CanSat after deployment. To achieve this, a servomotor was used, which, when activated, rotated a component to which the flag was attached, thus forming the separation mechanism. Since there were no restrictions regarding the flag material, a piece of an alpaca wool garment with the name "Perú" engraved was used.

SYSTEM DESIGN

System design is a fundamental part of the project development, as exemplified in Fig. 1, since it encompasses the payload necessary to fulfill the defined missions. This process is directly related to the mission requirements, allowing for the establishment of the structure, component distribution, and the mechanisms needed in the mechanical system. Additionally, the sensors, actuators,



Source: Elaborated by the authors.

Figure 1. General block diagram of the project development stages.



batteries, and communication modules that make up the electrical and electronic system are identified and selected. Finally, the design includes data collection, analysis, and the transmission of signals through the telemetry system.

Based on these definitions, the workflow is developed in the following stages. First, the "structure integration" is performed, where the components are assembled following the previously established design, ensuring that the structure meets the size and weight constraints set by the competition. Additionally, suitable materials are selected to ensure the mechanical strength of the system. In the second stage, "evaluation, testing, and correction," the functionality and integration of the systems are verified. This includes testing sensors, communication, vibration resistance, mechanism deployment, and launch simulations. For example, a preliminary test is conducted using a cylindrical compartment to release the CanSat from a height of 15 meters, emulating deployment conditions. Errors identified during these tests are corrected, and the system is re-evaluated until optimal performance is achieved. Subsequently, in the "final prototype and launch" stage, the final prototype is prepared and ready for the competition. The official launch is carried out from a height of 150 meters using a drone provided by the event organizers. Finally, in the "data collection and analysis" stage, the collected information is analyzed, such as the angular variation of the CanSat during flight, the final position relative to the target, and the effectiveness of the biodegradable liquid release mechanism during descent.

MECHANICAL SYSTEM

Structure

The CanSat features a cylindrical structure designed to minimize aerodynamic resistance and evenly distribute mechanical stresses, optimizing its stability compared to other geometric configurations. Part of the structure is divided into three compartments, each designed to house systems, mechanisms, and electronic components according to their function. These compartments are the upper compartment, the cylindrical compartment, and the battery compartment. The complete structure is made up of several independent components that, when assembled, form a cylinder with a height of 200 mm and a diameter of 80 mm. Each component was precisely modeled using the Autodesk Inventor 2024 software, ensuring the exact integration of all parts. The main features of each compartment are described below, along with the specific mechanisms they incorporate and their function within the system.

- Upper compartment First, this compartment is responsible for holding the parachute. It includes holes that allow airflow to pass through, facilitating its early release. Additionally, it features an opening on its top to place a magnetometer. The entire structure is mounted on 200 mm rods, 3D printed using polycarbonate (PC) material, and secured with nuts at the bottom of the base platform, as well as at the four largest holes of the compartment to ensure proper alignment. The rods have a 10 mm thread at each end, created with a 3/16" tap, allowing the nuts to be easily adjusted. The compartment also has a rectangular opening on the side to accommodate the system that will release a flag using the flag release mechanism, in which the servomotor mount is placed. The compartment was printed using silver-colored polylactic acid (PLA) 3D printing material.
- Cylindrical compartment It is located beneath the upper compartment and houses two circular printed circuit boards (PCBs), named PCB-1 and PCB-2 according to their function. Each of them has a diameter of 75 mm and four 4.5 mm holes to allow the passage of the rods. Both are secured within this compartment by a support at the top for PCB-1 and a PC-printed piece that holds PCB-2, ensuring their proper placement without obstruction.
- Battery compartment It is located in the lower half of the structure and serves the purpose of housing two batteries that provide the necessary power for the CanSat to fulfill its missions. This compartment is divided into two sections. The first section has two openings that allow the upper part of the batteries to be fitted. Below this, there is a designated space for the piece that holds the motor responsible for driving the worm screw, which activates the vertical descent mechanism. Beneath this piece, there are supports for the two MG90S servomotors, which control the arms and enable descent control by directing the parachute.

The second section is similar to the first but includes two additional rectangular openings: one for the CanSat's power switch and another for charging the batteries, facilitating recharging without the need to disassemble the structure.



Finally, at the bottom of the structure, the liquid release mechanism and the vertical descent mechanism are located. The latter consists of four cylindrical supports, 3D printed in PC, which separate the battery compartment from the circular support of the worm gear system. This configuration ensures that upon landing, the support of the worm gear system remains stable and fixed. The components holding the liquid-filled balloons have a curvilinear shape designed to direct the liquid toward the center when the balloons break. To achieve this, a PC-printed piece is used, attached to the lower part of the worm screw. In this way, both mechanisms (vertical descent and liquid release) are activated simultaneously, ensuring that the four supports do not interfere with the liquid release.

Vertical descent mechanism

It is designed to achieve a vertical landing using four 55 mm long supports, whose design resembles a claw, providing stability and resistance. At the bottom of these supports, there are four shock-absorbing springs attached to four thermoplastic polyurethane (TPU) 3D-printed suction cups, which help improve adhesion to the surface, while the springs cushion the impact of the landing. Each support, printed in PC, is connected to a 20-tooth resin gear via four screws. The gear has been modified with an extrusion that allows the screws to secure the supports and their respective gears, facilitating the handling of components in case of damage or replacement. The rotation of the worm screw enables the movement of the joint between the gear and the support.

The gear-support assembly is attached to a circular support with a diameter of 75 mm using four bolts and nuts, ensuring stability during rotation. A Pololu direct current (DC) motor, specifically the 6 V high power (HP) metal micro-gearmotor, is attached to the structure to maintain its vertical position and drive the double-helix worm, which causes the four crowns connected to the supports to rotate around an axis perpendicular to that of the screw. The transmission of motion from the DC motor to the worm screw is achieved through a 3 mm hexagonal coupling, which is connected to the worm screw using a 30 mm long M4 screw. In this way, the rotation generated by the motor is transferred to the worm screw and then to the gears through a simple connection between the components.

Liquid release mechanism

It is integrated with the worm screw, as they share the same axis connected to the DC motor. The liquid used in this system was the Peruvian national drink, *chicha morada*, stored in balloons. The release system is activated simultaneously with the vertical descent mechanism. During activation, needles attached to a PC-printed component begin to rotate, allowing them to puncture the balloons, releasing the liquid and creating visible marks on the impact surface.

Flag release mechanism

This mechanism uses a 2.5 mm diameter, 40 mm long rod as the flagpole. The rod is mounted on a PC-printed component, which includes a cavity designed to securely hold one end of the rod. The printed component not only secures the rod but also includes a hole at the opposite end to attach it to an MG90S servomotor using a small screw. In its initial position, the system keeps the flagpole pointing downward. When the servomotor is activated, it rotates the assembly, raising the rod until the flagpole points upward with the flag. This movement ensures the flag is properly oriented during flight and after landing.

The entire assembly is mounted on a servomotor support, designed and 3D-printed in acrylonitrile butadiene styrene (ABS) material. The support has two holes, one for the passage of the rods and the other for adjustment at the top of the CanSat. The position of the flag release system is chosen to avoid interference with the arms and supports during its release.

Arm mechanism

The system incorporates two MG90S servomotors and an additional servomotor to raise the flag. These servomotors are activated based on commands from the microcontroller. Due to the high torque required by the glider, the servomotors are equipped with metal gears, making the MG90S model suitable for a maximum torque of 2.5 kg·cm. The system connects each MG90S servomotor through 3-pin connectors, providing both power and signal. The two servomotors are mounted on the sides of the CanSat using 3D-printed PC material supports, which, like the flag release mechanism, have holes for the passage of the rods.

Each servomotor is equipped with arms also 3D-printed in PC, which play a key role in controlling the glider. These arms are attached to the servomotors with small screws. Through their connection to the glider's control lines, these arms apply tension to adjust the direction and turn during flight. As the servomotors move, the tension in the lines changes, which, in turn, modifies the glider's trajectory.



The arm's control mechanism is integrated with a GPS module that provides position information, essential for navigation. This GPS data serves as feedback to the flight control system, ensuring the CanSat maintains its planned trajectory and allowing for autonomous adjustments.

PARAGLIDER DESIGN

When the CanSat is released, it is subject only to the action of two main forces: gravitational force and aerodynamic drag, the magnitude of which depends on the geometric and structural characteristics of the glider (Saez date unknown). The latter has evolved from basic parachute designs to more advanced configurations, optimized to efficiently take advantage of both thermal and dynamic updrafts, enabling sustained flight without an engine (López Laval *et al.* 2019). By utilizing the aerodynamic profile of the wing, the glider can capture the updrafts generated by thermal gradients (thermal currents) and the dynamic lift caused by the interaction of airflow with the terrain. Since gliders do not have engines, pilots rely on atmospheric effects to control their flight. In still air, a glider constantly descends; therefore, to extend flight time, pilots use thermals to ascend. These thermals are regions of upward-moving air generated by temperature differences, causing the air to flow from warmer to cooler zones. During flight, pilots constantly search for areas with favorable thermal characteristics to climb and gain altitude (Wirz *et al.* 2011). This allows them to maintain altitude and maneuverability for extended periods. This is the main reason for using it in the project, as it must follow a desired trajectory to meet the missions required by the competition. Calculation of the projected area takes into account the maximum terminal velocity required for the CanSat France 2024 competition, set at 5 m·s. The terminal velocity depends on certain parameters such as: projected area, glider shape, drag coefficient, air density, gravity, payload mass, and wind velocity. The projected area is calculated using the terminal velocity equation:

$$v_{\infty} = \sqrt{\frac{2mg}{\rho A C_D}} \tag{1}$$

where V_{∞} is the terminal velocity (5 m·s), m is the mass (800 g), g is the acceleration due to gravity (9.81 m·s²), ρ is the air density (1,204 kg·m³), A is the cross section of the paraglider (0.66 m²), and C_d is the drag coefficient.

Due to the small size of the CanSat device, a 9-cell paraglider was chosen to avoid the complexity in its manufacturing and the structure of the lines attached to its body. The paraglider fabrication process consists of 3 stages: (i) mold fabrication using a software called "SingleSkin version 0.3," which, using the projected area parameter and number of cells, provides the final design of the cells and ribs; (ii) the fabrication of the cells and ribs from a high tear-resistant fabric, in this case, Ripstop nylon, followed by their assembly; and (iii) finally, the rope system, which is made of braided nylon, is installed, running from the glider to the body of the CanSat and its arms. These stages are illustrated in Fig. 2.

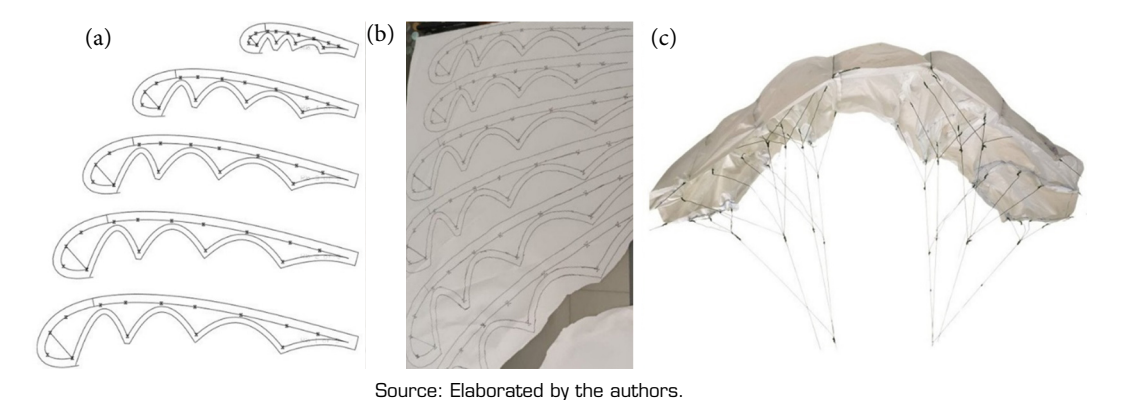


Figure 2. Three stages of paraglider manufacturing; a) mold manufacturing; b) creation of cells and ribs; c) installation of the rope system.



ELECTRICAL AND ELECTRONIC SYSTEMS

The system's electronics consisted of an Arduino Nano 33 BLE development board, sensors, a GPS module, a RF module, a motor controller (H-bridge), and three servomotors. The general power supply for these peripherals was primarily provided by two batteries of 3.7 V with a charge of 2,000 mAh each. These batteries were connected in series, providing an input voltage to the system of 7.4 V with 2000 mAh. The direct power supply to the peripherals was provided by regulators that supplied 5 V and 3.3 V as required by each sensor.

The data transmitted through the system's electronic peripherals was done using I2C, SPI, and UART communication protocols. The data was received by the microcontroller, which processed the signals to determine control and data transmission (via the RPSMA XBee3 module).

The control peripherals consisted of the Sparkfun GPS Breakout SAM-M8Q module and two MG90S servomotors. The microcontroller captured the real-time position through the GPS module, and based on that current location, the electrical signals sent to the servomotors were determined using the Pulse Width Modulation (PWM) technique. Sensor Subsystem

The integration of all electronic devices at the hardware level was carried out by developing two electronic boards that contained the sensors described in Table 1.

Sensor no. Sensor **Brief description Observations** A temperature sensor integrated into the Arduino Measures the temperature in real time as the 1 HTS221 board with a measurement range of 15-40 °C, system descends with an accuracy of O.5 °C An absolute pressure sensor integrated into the It measures the pressure at which the value of the 2 LPS22HR peak height of the satellite is obtained through a Arduino board with a measurement range of 260-1,260 hPa linear relationship With this sensor, it is possible to determine Sensor integrated into the Arduino board with dynamic magnitudes of the device, such as speed, 3 LSM9DS1 three acceleration channels, three angular velocity acceleration, and magnetic field, in the three axes channels, and three magnetic field channels (X, Y, and Z) DC sensor with a range of O-3.2 A with a precision It determines the current consumed by the entire 4 INA219 of 0.8 mA system It determines the orientation of the CanSat 5 HMC5883L 3-axis magnetometer concerning the Earth's magnetic field to orient the device

Table 1. List of system sensors.

Source: Elaborated by the authors.

The first board (PCB-1) integrated components such as: the Sparkfun GPS Breakout SAM-M8Q module, the microSD module, the RPSMA Xbee3 radiofrequency module, as well as a voltage regulator from 5 to 3.3 volts, which provided power for the GPS and microSD modules, and connectors that established both communication and power supply input to PCB-1 (Moreno *et al.* 2025), as well as output for controlling devices such as the servomotors and the motor coupled to the worm screw.

The second board (PCB-2) integrated components such as the INA219 module, the MX1508 module, and connectors that established communication between both boards, in addition to power input and output. The power input for the entire system was provided through a connector at a voltage of 7.5 volts. This board also housed a 5-Volt regulator, which supplied power to the INA219 and the devices on PCB-1 through a connector. The power supply for the servomotors was set to 7.5 volts through a connector that branched from PCB-2 to PCB-1.

COMMUNICATION AND POSITIONING SUBSYSTEM OF THE CANSAT

The communication system was based on an XBee3 RPSMA RF module, which provided robust and reliable long-distance communication. This module operated in the 2.4 GHz frequency band with a maximum power of 20 dBm and communicated



with PCB-1 via the USART protocol. On the other hand, the real-time geolocation of the CanSat was achieved using a Sparkfun SAM M8Q GPS module, which operated in the L1 satellite band at 1,575.42 MHz and allowed a maximum altitude measurement range of 50 km. The communication protocol of this device was I2C.

ELECTRICAL POWER SUBSYSTEM

The power system consisted of two 3.7-volt batteries, each with a capacity of 2,000 mAh, which, when connected in series, provided a net voltage of 7.4 V to the system. The choice of batteries was based on the average current consumption of the entire system, which is primarily determined by the servomotors and the DC motor, as these components set the maximum current demands. The CanSat required a minimum current of 225 mA, an average current of 340 mA, and a maximum current of 3 A. DC-DC regulators were necessary as they provided a safe and reliable power source for the sensors and other devices in the picosatellite. The AMS1117 and LM2596 voltage regulators were designed to regulate voltage to 3.3 V and 5 V, respectively, for powering the devices. Figure 3a illustrates how the voltages are regulated within the system. For battery recharging, a 3-pin charging connector was used, located on the side of the CanSat. Figure 3b shows this connection diagram. To charge the battery, it was necessary to deactivate the main power source, and charging was not carried out simultaneously.

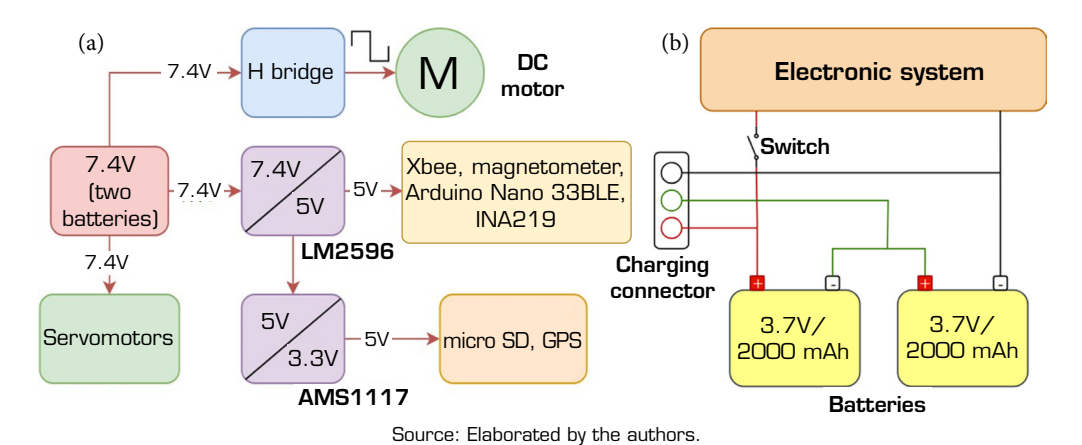


Figure 3. Block and connection diagram for voltage regulation in the system (a) and battery charging (b).

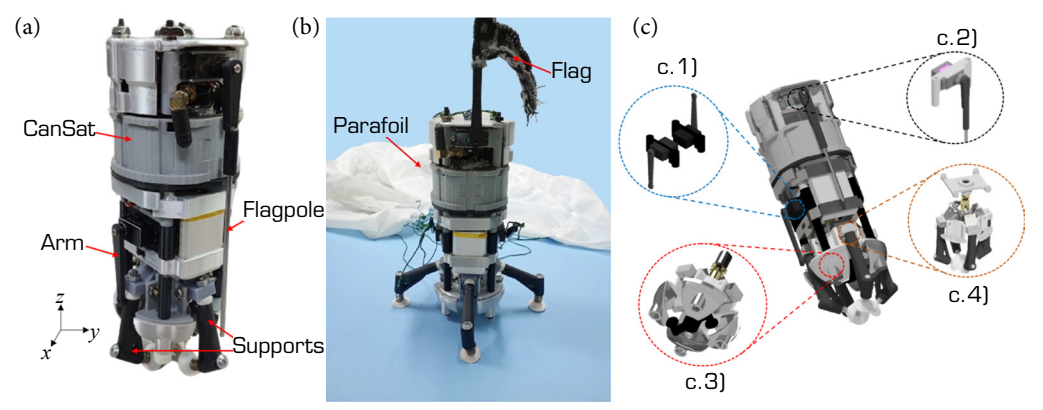
EVALUATION TEST, LAUNCH, AND DISCUSSIONS

Figure 4a shows the complete mechanical configuration of the CanSat, with the mast pointing downward, the vertical arms, and the supports not deployed. In Fig. 4b, the flag, glider, and supports are shown fully deployed. Additionally, Fig. 4c provides a detailed view of the mechanisms, highlighting their arrangement within the assembly and the design features that allow for proper operation.

COMMUNICATION TEST

The GPS module code was programmed using an Arduino Nano microcontroller to obtain the latitude and longitude of the testing location and test the module's communication before integrating it into the CanSat. To achieve good results, the GPS was placed in a location with minimal interference, such as away from metal structures, dense trees, or electronic devices that could affect the signal, and not under any infrastructure, as mitigating these effects is essential to maintaining the accuracy and reliability of the GPS (Deshpande 2004).





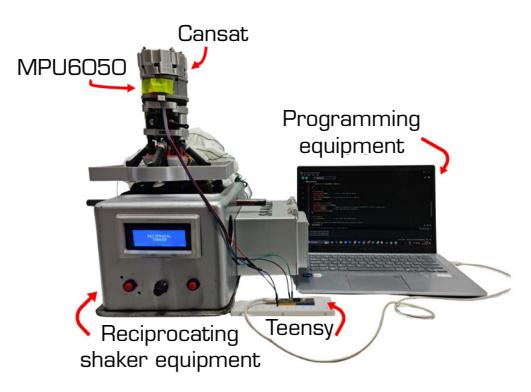
Source: Elaborated by the authors.

Figure 4. Overview and details of the CanSat mechanisms. (a) mechanical configuration of the CanSat; (b) flag, vertical supports, and parafoil deployed; (c) mechanisms for arms (c.1), flag release (c.2), liquid release (c.3), and vertical descent (c.4).

A few minutes were allowed for the GPS to acquire the satellite signal and improve location accuracy. The GPS managed to connect with seven satellites, facilitating the acquisition of the coordinates determined by the code in Arduino. To verify accuracy, the obtained latitude and longitude coordinates were entered into Google Maps, which showed an error of approximately 7 meters between the measured location and the actual location. According to the u-blox SAM-M8Q module datasheet, the typical horizontal accuracy under optimal conditions is 2.5 meters (Durler 2024). However, with interference (buildings or trees) or in adverse conditions with few satellites, the error increases to 5 to 10 meters or more. According to this, the error of 7 meters is within the appropriate range, so the GPS operation and measurement were considered correct. In addition to the GPS module, communication between the XBee modules used in CanSat was verified to be stable. To test this, Digi XCTU software was installed for data transmission between the XBee modules. To monitor communication, random data was transmitted between both modules, increasing the distance to 100 meters to confirm wireless communication. After performing individual tests on the communication and data transmission modules, their operation was again verified on the integrated CanSat, which was moved to the top floor of a five-story building, while the ground station remained at the bottom of the building. Through communication with the XBee, commands were sent to open the CanSat cradles, thus ensuring the correct transmission and reception of instructions.

VIBRATION TEST

This test aims to ensure that the KunturSat's electronic and mechanical components remain assembled and can withstand the vibrations generated during launch. It also verifies the proper functioning of the sensors and, in particular, the XBee communication for data transmission. Figure 5 shows the experimental setup for the vibration test, which used a Tabof brand linear reciprocating



Source: Elaborated by the authors.

Figure 5. Experimental configuration of the reciprocating shaker equipment.



shaker. This device generates an oscillatory motion in a single direction, moving back and forth along an axis, allowing vibrations to be simulated at different frequencies. The MPU6050 sensor was used to detect motion and measure acceleration. A Teensy 4.1 microcontroller, programmed in Arduino, was also used to acquire acceleration data.

The test was carried out at five programmed vibrator frequencies (3.40 Hz, 3.58 Hz, 3.75 Hz, 3.92 Hz, and 4.15 Hz), and at each of them, the MPU6050 sensor allowed direct measurement of the vibration experienced in the CanSat.

Figure 6 shows the acceleration amplitude versus frequency graph, created using MATLAB software. A higher amplitude indicates intense vibrations, while a lower amplitude suggests milder vibrations. As the frequency increased, the CanSat's operation was verified. If it failed, the connections were reinforced, and the mechanism was adjusted to improve stability. Furthermore, it was ensured that the vibrations would not break the balloons filled with biodegradable liquid (chicha morada).

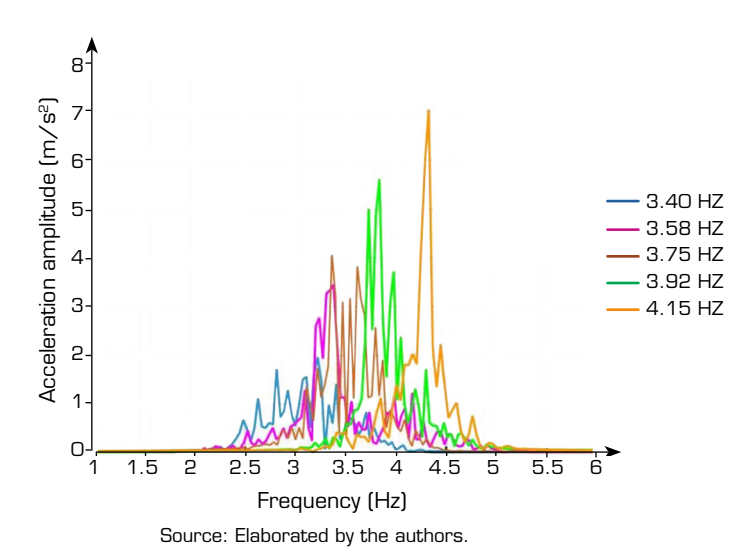


Figure 6. Graph of acceleration amplitude as a function of frequency.

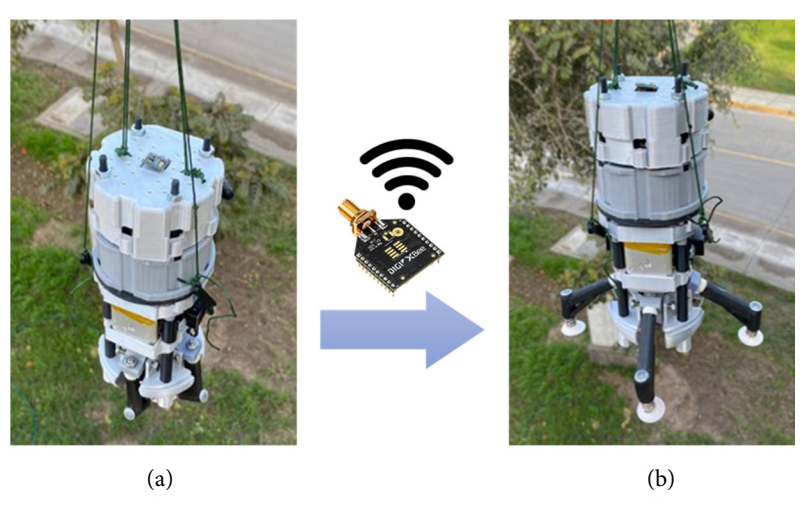
Experimental tests showed that the CanSat can withstand accelerations of up to 7 m·s² (Fig. 6), which was the limit measured in the tests. This result validates its ability to withstand the vibrations induced during the vibration test and during the acquisition of data in free fall when the paraglider is deployed, since while it opens and stabilizes the descent speed, the acceleration is less than or equal to the acceleration due to Earth's gravity (9.81 m·s²) and when it is open, the net acceleration is close to zero due to the balance between the weight of the CanSat and the drag force of the air (Libii 2007).

SUPPORT OPENING THE TEST

The CanSat has a landing system with four supports to keep it in a vertical position. The objective of this test is to measure the time required to determine the number of seconds required for the extensions to open correctly and completely to support the picosatellite.

As shown in Fig. 7, these supports are initially close together, keeping the system closed. A signal is sent through the XBee modules to open them (Fig. 7b), allowing the CanSat to remain vertical. For this test, it was verified that the landing supports deployed correctly upon receiving the telemetry signal. Once this stage was validated, an opening time of 2 seconds was determined, which allowed the CanSat's base to be widened, better distributing the weight and reducing pressure, which helped minimize the risk of tipping.





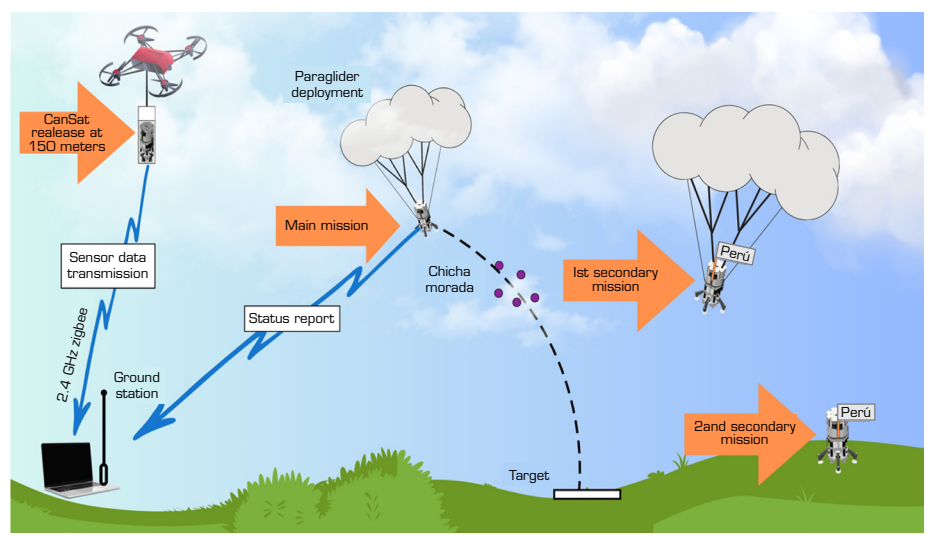
Source: Elaborated by the authors.

Figure 7. Testing the opening of the CanSat supports without deploying (a) and deployed (b).

PRE-RELEASE TESTING

The test simulated the launch of the CanSat and its release from a container (Annex) designed for the competition, with the aim of ensuring proper deployment of the paraglider. It was designed with dimensions according to the competition requirements, with 9.5 cm in diameter and 30 cm in height, an Arduino, four batteries, and a servomotor, which actuates a lever to release the lid and eject the picosatellite after 10 seconds of activation. During the initial launches, several failures prevented the paraglider from opening, leaving it stuck inside the container. However, the problem was resolved by starting the folding process from the center, folding it several times, and rolling it up to prevent blockages. The lines were also untangled before each test to prevent in-flight failures. It was observed that the impact was less severe when the paraglider was deployed correctly from the intended altitude, and that the sensors and data transmission functioned properly during the descent.

The flight results were obtained at the camp facilities in France, where a primary mission and two secondary missions were carried out: flag deployment and vertical positioning on the ground. Figure 8 illustrates the stages of the flight, from initial preparation



Source: Elaborated by the authors.

Figure 8. Flight plan: mission stages and payload deployment.



to landing. The KunturSat was placed in a 95 mm diameter and 300 mm high container, then activated and its data transmission verified before being released from a drone at 150 meters altitude. During the descent, purple corn drink was released, allowing the internal balloons to detonate and the supports to deploy for vertical descent, while telemetry was sent to the ground station. Finally, the flag was deployed, marking the end of the descent. The entire flight lasted 46.6 seconds, with a descent rate of 4.55 m·s, and telemetry was recorded at an altitude of 100 meters. The launch test was conducted around 11:00 h.

BATTERY TEST

Two LiPo batteries were used to power the KunturSat. In this test, the objective was to ensure that the LiPo batteries had the capacity and minimum duration of 45 minutes, according to rule 11 of the CanSat France 2024 competition (C'Space 2024), to supply power to the picosatellite during the mission. For this purpose, a TC4056 1A LiPo battery charger with a Type-C controller was used, which was used for half an hour for each battery, enough time to fully charge them. The batteries were then placed in the CanSat to provide power for approximately 1 hour to the integrated picosatellite. During this hour of testing, it was verified that the sensors continued to function correctly and that data transmission remained operational and uninterrupted. According to the EPS section, the average consumption of the CanSat is approximately 340 mA and the capacity of each battery is 2,000 mAh (Fig. 3b), so the theoretical operating time is $2,000/340 \approx 5.88$ hours, which confirms that the autonomy of a minimum of 45 minutes was widely guaranteed.

MAIN MISSION

Figure 9, created using MATLAB software, shows the evolution of the distance between KunturSat and the ground target over time. Initially, a countdown period is observed during the first 10 seconds, followed by the launch of KunturSat at 11.2 seconds. During its descent, the liquid (purple corn drink) was released at second 40.2, at which point the system's state changed from low to high. After the release, KunturSat continued its trajectory, progressively moving away from the target at 125.520 cm, thus concluding its flight.

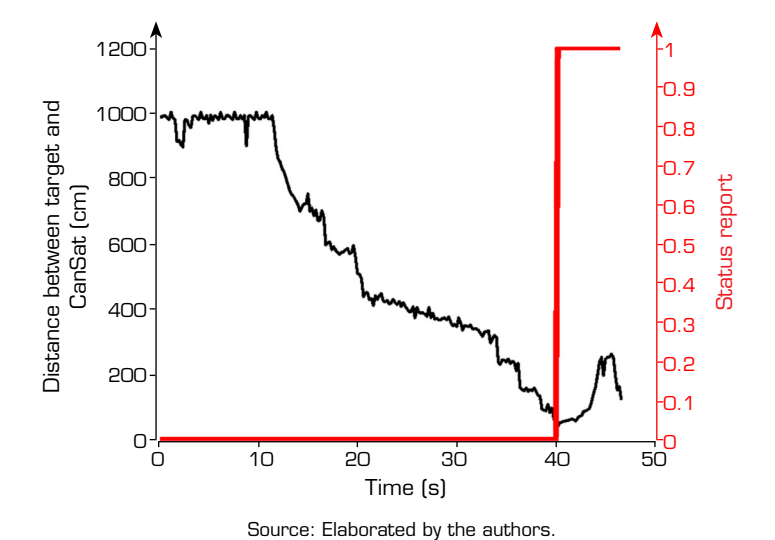


Figure 9. Distance between KunturSat and the target during the landing sequence.

FIRST SECONDARY MISSION: MAINTENANCE OF VERTICAL POSITION

The vertical positioning mission began with the deployment of the stabilizing supports, the objective of which was to ensure that the system landed and remained in a vertical position. As shown in Fig. 10, created using the MATLAB software, the angular



variation curves were recorded throughout the flight by the IMU sensor, which constantly monitored the CanSat's Pitch and Roll axes. The final angular variations reached 85.11° on the Pitch axis and 11.52° on the Roll axis, indicating a considerable inclination but within the expected limits for the final stability of the system.

The graph reveals a sharp increase in angular variations shortly after launch, at approximately 10 seconds, due to the release of the CanSat and the subsequent deployment of the parachutes, followed by stabilization around 16 seconds into the flight. The drop in angular values at 45 seconds coincides with landing, suggesting that the system fell at an angle and was unable to fully descend vertically. The attached image shows the final position of the CanSat.

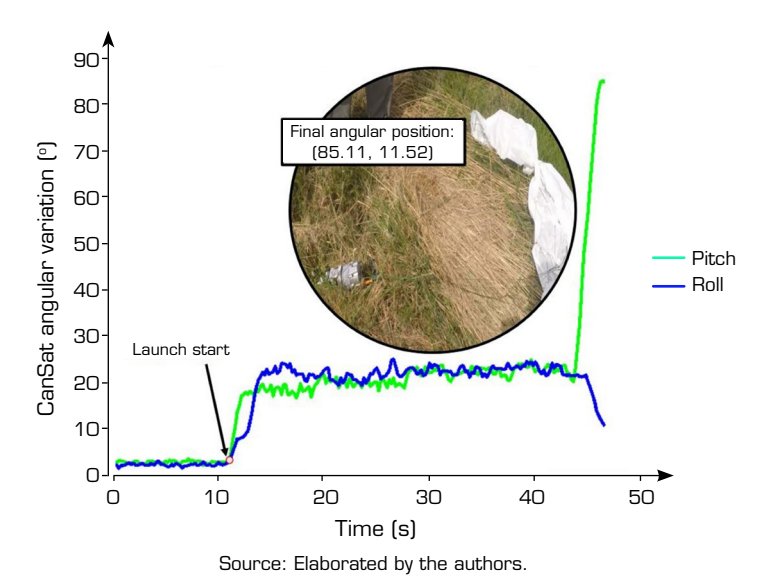


Figure 10. Angular variation of CanSat during flight and final position after landing.

SECOND SECONDARY MISSION: FLAG DEPLOYMENT

The picosatellite's approach condition, with a 50 cm discrepancy from the target point programmed in the microcontroller, was successfully achieved, demonstrating that the flag deployment worked simultaneously with the supports during the flight. Figure 11 captures the moment when both the vertical descent and flag release mechanisms were activated.



Source: Photograph by the C'Space event team.

Figure 11. KunturSat flight deployment.



CONCLUSION

This article presents a comprehensive development of the KunturSat picosatellite, designed for the CanSat France 2024 competition, showcasing innovation in mechanisms and systems that precisely address the specific challenges of the competition. KunturSat's structural design not only meets the competition's constraints but also introduces advanced systems for flag release and descent control via a 9-cell paraglider, ensuring a controlled terminal velocity and precise landing in the target area. These components were optimized using materials such as Ripstop nylon and advanced 3D printing techniques, enabling a lightweight and durable construction.

The study also highlights the project's eco-friendly approach by implementing a purple corn drink delivery system, a biodegradable liquid used as a landing zone marker. This innovative approach demonstrates a commitment to sustainability by integrating solutions that reduce environmental impact during testing and real-life missions. Furthermore, modeling software such as Autodesk Inventor facilitated the simulation and validation of the mechanisms, ensuring their effectiveness under competitive conditions. However, areas for improvement were identified, particularly regarding the need to reinforce certain critical design points to increase durability and resilience under adverse conditions. In terms of its technical contribution, KunturSat stands out as a valuable educational and research platform for the development of future picosatellites. The integration of advanced design and manufacturing techniques, along with a focus on functionality and precision, positions this project as a benchmark in the aerospace field, particularly for those seeking innovation in controlled descent systems and suborbital satellite release mechanisms.

In essence, the work on KunturSat represents a significant contribution to the field of satellite technology, demonstrating the viability of innovative and environmentally friendly approaches to space missions.

CONFLICT OF INTEREST

Nothing to declare.

AUTHORS' CONTRIBUTION

Conceptualization: Moreno LFA, Orellana JMV, Adriano MAR, Tarazona FR, Meza KKR, and Alta RYP; Software: Moreno LFA, Orellana JMV, Adriano MAR, Tarazona FR, and Meza KKR; Validation: Moreno LFA, and Alta RYP; Formal analysis: Moreno LFA and Meza KKR; Investigation: Moreno LFA, Orellana JMV, Adriano MAR, Tarazona FR, and Meza KKR; Resources: Moreno LFA and Alta RYP; Data Curation: Moreno LFA, Adriano MAR, and Meza KKR; Writing – Original Draft: Moreno LFA, Orellana JMV, Adriano MAR, Tarazona FR, and Meza KKR; Writing – Review & Editing: Alta RYP and Orellana JMV; Visualization: Moreno LFA, Orellana JMV, Adriano MAR, Tarazona FR, and Meza KKR; Supervision: Alta RYP; Project administration: Moreno LFA and Alta RYP; Funding acquisition: Alta RYP; Final approval: Alta RYP.

DATA AVAILABILITY STATEMENT

Supplementary material: https://doi.org/10.6084/m9.figshare.29378831.v1

FUNDING

Vice-Rectorate for Research at the National University of Engineering Grant No: FC-PF-10-2022.



ACKNOWLEDGMENTS

Our sincere gratitude to Professor Dr. Walter Francisco Estrada López for his invaluable technical support, as well as his administrative and logistical assistance throughout the course of this project.

REFERENCES

Aly H, Sharkawy O, Nabil A, Yassin A, Tarek M, Amin SM, Ibrahim MK () Project-based space engineering education: application to autonomous rover-back CanSat. Paper presented 2013 6th International Conference on Recent Advances in Space Technologies. IEEE AESS, Aeronautics and Space Technologies Institute (ASTIN) Air Force Academy, Istanbul, Turkey. https://doi.org/10.1109/RAST.2013.6581164

Aydemir ME, Celebi M, Ay S, Vivas EV, Bustinza FC, Phan D (2011) Design and implementation of a rover-back CanSat. Paper presented 2011 5th International Conference on Recent Advances in Space Technologies. IEEE AESS, Aeronautics and Space Technologies Institute (ASTIN), Air Force Academy; Istanbul, Turkey. https://doi.org/10.1109/RAST.2011.5966952

Bhattarai S, Go JS, Oh HU (2021) Experimental CanSat platform for functional verification of burn wire triggering-based holding and release mechanisms. Aerospace 8(7):192. https://doi.org/10.3390/ AEROSPACE8070192

Botero Y, Lopez A, Restrepo S, Rodriguez JS, Valle D, Galvez-Serna J, Elkamel A, Amiraslani F, Yarce Botero A, Restrepo SL, et al. (2023) Design and implementation of a low-cost air quality network for the Aburra Valley surrounding mountains. Pollutants 3(1):150-165. https://doi.org/10.3390/POLLUTANTS3010012

Chun C, Tanveer MH, Chakravarty S (2023) The CanSat compendium: a review of scientific CanSats. Machines 11(7):675. https://doi.org/10.3390/MACHINES11070675

Contente J, Galvão C (2022) STEM education and problem-solving in space science: a case study with CanSat. Educ Sci 12(4):251. https://doi.org/10.3390/EDUCSCI12040251

[C'Space] (2024) Concours CanSat France 2024. Règlement – 18e édition. [accessed Feb 22 2025]. https://www.planete-sciences.org/espace/IMG/pdf/reglement_cansat_2025.pdf

Deshpande SM (2004) Study of interference effects on GPS signal acquisition (master's thesis). Calgary: University of Calgary.

Durler M (2024) SAM-M8Q Easy-to-use u-blox M8 GNSS antenna module data sheet. [accessed Feb 22 2025].www.u-blox.com

Kopacz JR, Herschitz R, Roney J (2020) Small satellites: an overview and assessment. Acta Astronautic 170:93-105. https://doi.org/10.1016/J.ACTAASTRO.2020.01.034

Libii JN (2007) The determination of the aerodynamic drag force on a parachute. World Trans Eng Technol Educ 6(1):1-4.

López Laval I, Sitko S, Plana Galindo C (2019) El parapente como deporte con interés científico: no solo traumatología. J Negat no Posit Results 4(6):644-656. https://doi.org/10.19230/jonnpr.3031

Millan RM, von Steiger R, Ariel M, Bartalev S, Borgeaud M, Campagnola S, Castillo-Rogez JC, Fléron R, Gass V, Gregorio A, et al. (2019) Small satellites for space science: a COSPAR scientific roadmap. Adv Sp Res 64(8):1466-1517. https://doi.org/10.1016/J.ASR.2019.07.035

Moreno LA, Alta RP, Lopez WE (2023) Precession motion of a CanSat rover-back prototype during its fall-to-Earth descent. Paper presented 2023 IEEE Latin American Electron Devices Conference. IEEE; Puebla, Mexico. https://doi.org/10.1109/LAEDC58183.2023.10209111



Moreno LF, Orellana JM, Adriano MA, Tarazona F, Meza KK, Alta RY. KunturSat: Design and development of a picosatellite for the CanSat France 2024 Competition [supplementary material]. Figshare; 2025. https://doi.org/10.6084/m9.figshare.29378831.v1

Nag S, Lemoigne J, De Weck O (2014) Cost and risk analysis of small satellite constellations for Earth observation. Paper presented 2014 IEEE Aerospace Conference. IEEE; Big Sky, USA. https://doi.org/10.1109/AERO.2014.6836396

Saez G (date unknown) Manual básico del parapentista. [accessed Feb 15 2025]. https://www.ultraligero.net/E_Books/manual_del_parapentista_paragliding_paramotor.pdf

Song Y, Gnyawali D, Qian L (2024) From early curiosity to space wide web: the emergence of the small satellite innovation ecosystem. Res Policy 53(2):104932. https://doi.org/10.1016/J.RESPOL.2023.104932

Swayampakula SSRK, Vedangi KV, Panangipalli VK, Gummadavelli M, Mala N, Banavath MN, Paladugu N, Kallem A (2024) Design and development of a CanSat for air pollution monitoring with RSSI-based position retrieval system. Adv Sp Res 75(9). https://doi.org/10.1016/J.ASR.2024.02.042

Sweeting MN (2018) Modern small satellites: changing the economics of space. Proc IEEE 106(3):343-361. https://doi.org/10.1109/JPROC.2018.2806218

Urquizo Cruz EP, Sánchez Salcán NJ (2019) Extracto del maíz morado como indicador químico. Chakiñan, Revista de Ciencias Sociales y Humanidades 9:45-57. https://doi.org/10.37135/chk.002.09.08

Wirz M, Strohrmann C, Patscheider R, Hilti F, Gahr B, Hess F, Tröster G (2011) Real-time detection and recommendation of thermal spots by sensing collective behaviors in paragliding. Paper presented 2011 1st International Symposium from Digital Footprints to Social and Community Intelligence. ACM; Beijing, China. https://doi.org/10.1145/2030066.2030070

Zhou C, Senadeera W, Wahia H, Kabutey A, Tsholofelo Nthimole C, Kaseke T, Amos Fawole O (2024) Exploring the extraction and application of anthocyanins in food systems. Processes 12(11):2444. https://doi.org/10.3390/PR12112444

